CHIN. PHYS. LETT. Vol. 35, No. 7 (2018) 072301

Theoretical Prediction of Diamond Betavoltaic Batteries Performance Using ^{63}Ni *

Yu-Min Liu(刘玉敏), Jing-Bin Lu(陆景彬)**, Xiao-Yi Li(李潇祎), Xu Xu(许旭), Rui He(何瑞), Ren-Zhou Zheng(郑人洲), Guo-Dong Wei(尉国栋)

College of Physics, Jilin University, Changchun 130012

(Received 26 March 2018)

A diamond p–n junction is used to convert the decay energy of ^{63}Ni source into electrical energy. The self-absorption effect of the ^{63}Ni source, the backscatter process and the transport process of beta particles in diamond materials are studied. Then the theoretical maximum of electrical properties and the energy conversion efficiencies of diamond-^{63}Ni p–n junction batteries are achieved. Finally, a feasible design of $p^+p^-n^+$ junction battery, which has the maximum output power density of 0.42 $\mu W/cm^2$ and the optimal device conversion efficiency of 26.8%, is proposed.

PACS: 23.90.+w, 23.40.−s, 88.80.ff, 84.60.−h DOI: 10.1088/0256-307X/35/7/072301

In recent decades, betavoltaic batteries have been investigated using theoretical calculations and experimental tests.[1−16] A betavoltaic battery mainly contains the beta source and the energy converters such as p–n junction, p–i–n junction and Schottky barrier diodes.[2] When beta particles interact with the energy converter material, the electron-hole pairs, which generate in or near the depletion region, can be separated by the internal electrical field and then collected for the radiation-induced current formation.[1,2] Thus the decay energy is converted into electrical energy directly. Compared with micro-chemical cells and micro-solar cells, the advantages of betavoltaic batteries mainly include easy integration in small scale, long service lifetime, high energy density and slight maintenance.[2−8] Therefore, betavoltaic micro-cells have become promising micro-power sources for the micro-electronic mechanical systems (MEMS) such as wireless networks and temperature sensors.[2−8]

The previous studies on betavoltaic batteries have been extensively reported on Si,[3−5] GaAs,[5,6] SiC,[7−9] GaN,[10−12] and ^{3}H,[9] ^{35}S,[1] ^{63}Ni,[4−16] ^{147}Pm,[2,5,13] ^{90}Sr/^{90}Y.[1,2,13] More recently, diamond betavoltaic batteries were demonstrated and most of the researches focused on the Schottky barrier-based batteries.[13−15] For example, in 2015, the experimental scCVD diamond Schottky barrier batteries were tested. The beta sources (^{63}Ni, ^{147}Pm and ^{90}Sr/^{90}Y) were used and the device conversion efficiency was up to 6%.[13] In 2016, an scCVD diamond p-doped/intrinsic/metal (PIM) membrane battery was tested by the electron beam induced current (EBIC) method. An open-circuit voltage of 1.85 V, a short-circuit current of 7.12 μA and the device conversion efficiency of 9.4% were measured when the electron beam energy was 20 keV.[14] However, there has been no experimental report on diamond p–n junction batteries except some theoretical researches. For example, in 2015, a diamond-^{63}Ni p–n junction battery was simulated using the Monte Carlo method. The device conversion efficiency of 29% was calculated when the thickness of the source was 6 μm.[16] In this study, based on Monte Carlo simulations, a theoretical prediction on the performance of diamond-^{63}Ni p–n junction batteries is achieved. Moreover, a feasible design of $p^+p^-n^+$ junction battery, which has the maximum output power density of 0.42 μW/cm^2 and the optimal device conversion efficiency of 26.8%, is obtained. Some physical parameters of the ^{63}Ni source and the diamond material are listed in Table 1.

Table 1. Parameters of the ^{63}Ni source and the diamond material.

^{63}Ni source	$T_{1/2}$ (a)	E_{ave} (keV)	β_{max} (keV)
	100.2	17.4	66.7
Diamond material	ρ (g·cm^{-3})	E_g (eV)	n_i (cm^{-3})
	3.52	5.5	1×10^{-27}

The ^{63}Ni source is an appropriate candidate for betavoltaic batteries because of the pure beta radiation, long half-life ($T_{1/2}$) and the moderate average decay energy (E_{ave}).[4−16] Moreover, its maximum decay energy (β_{max}) is below the threshold energy of radiation damage in most semiconductor materials.[2] For the diamond material, the advantages, which mainly include wide band gap (E_g), low intrinsic carrier concentration (n_i), low atomic number, high electron density, excellent electrical properties, temperature stability and chemical inertness, contribute to the high energy conversion efficiency and the stable performance of diamond-based batteries.[2,13−15] The diamond material has also exhibited very high radiation resistance even to the strong flux of high energy particles in detectors.[13] Furthermore, it is known that the electron-hole pairs are generated as well as heat in the interaction of beta particles with the semiconductor materials. The fraction of energy that goes into electron-hole pair formation in the matter is calculated as the ratio of band gap (E_g) to the mean ionization energy (E_{ehp}) and it is defined as the ultimate conversion efficiency of the material.[2] Here the mean ionization energy is confirmed as $E_{ehp} = 2.8E_g + 0.5$.[4] Then as shown in Fig. 1, the ultimate conversion efficiency

*Supported by the National Major Scientific Instruments and Equipment Development Project under Grant No 2012YQ240121, and the National Natural Science Foundation of China under Grant No 11075064.

**Corresponding author. Email: ljb@jlu.edu.cn

© 2018 Chinese Physical Society and IOP Publishing Ltd

increases and then nearly reaches the saturation value with the increasing band gap. For the diamond material, it is about 34.6%. Finally, it should be pointed out that the theoretical maximum of energy conversion efficiency of the cell, which is determined by the source, the transport process of beta particles in the matter and the energy converter, is different from the ultimate conversion efficiency of the material.

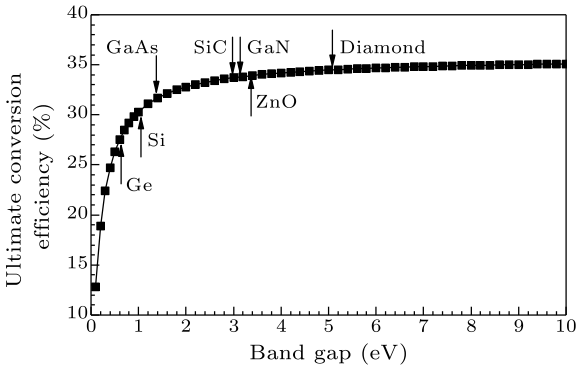

Fig. 1. The ultimate conversion efficiency versus band gap.

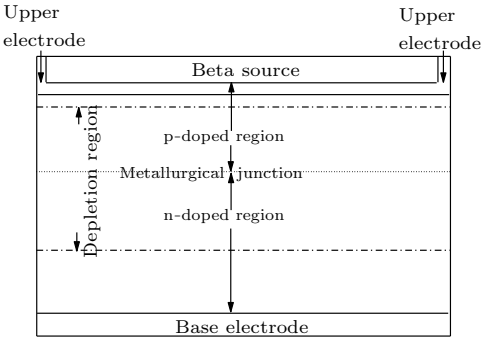

Fig. 2. The prototype of the p–n junction betavoltaic battery.

The typical prototype of the p–n junction betavoltaic battery is illustrated in Fig. 2. In this study, the structure of the p–n junction mainly includes a p^+ layer, a p^- layer and an n^+ layer.

It is known that when the beta particles traverse through the matter, the maximum of stopping power takes place at the surface and it decreases with the penetration depth increasing in the matter.[2,4] Moreover, the charge collection efficiency of electron-hole pairs generated in the depletion region is 100%. However, the electron-hole pairs generated outside the depletion region, which must diffuse into the depletion region as the minority carriers, can be separated and collected for the radiation-induced current formation. In general, the depletion region and its nearby regions, which are about one diffusion length of the minority carrier away from the edge of the depletion region, are refereed to as the active region in the betavoltaic batteries. Thus the p–n junction diode, whose depletion region can be designed to match the main ionizing radiation region, is the appropriate energy converter in a betavoltaic micro-battery. Currently, the depletion region of a practical p–n junction battery is usually smaller than the main ionizing radiation region.[2,4] To efficiently utilize the energy deposited outside the depletion region in a betavoltaic battery, the p-type doped region is selected as the emitter layer and the n-type doped region is used as the base layer. This design contributes to improving the charge collection efficiency outside the depletion region in the battery. The main reason is that the diffusion length of the electron is much larger than that of the hole under the same excess carriers density. For the diamond material, both electrons and holes have the high mobility rate and large diffusion length, which enables the low recombination rate of the generated electron-hole pairs even in the high doped region.[14] Furthermore, the high p-doped diamond layer, which has a low atomic number and excellent electrical properties, can be used as the entrance electrode layer in a diamond-based device.[14] The diamond electrode layer can also provide an electrochemical layer on which the radioactive isotopes can be directly precipitated.[14] Compared with the metal electrode layers such as Al, Ti, Pt, Au and Ni, the diamond entrance electrode layer results in the low energy backscatter loss and slight bremsstrahlung damage in the fabricated batteries.

In a betavoltaic battery, the short-circuit current density ($J_{\rm sc}$) is given by

$$J_{\rm sc} = \frac{\eta_{\rm CCE} \cdot q \cdot P_{\rm dep}}{S \cdot E_{\rm ehp}}, \tag{1}$$

where $\eta_{\rm CCE}$ is the charge collection efficiency, q is the unit electron charge, $P_{\rm dep}$ is the energy deposited in the active region, S is the junction area, and $E_{\rm ehp}$ is the mean ionization energy. Then the open-circuit voltage ($V_{\rm oc}$) is given by

$$V_{\rm oc} = \frac{k_{\rm B}T}{q} \ln\left(\frac{J_{\rm sc}}{J_0} + 1\right), \tag{2}$$

where $k_{\rm B}$ is the Boltzmann constant, T is the absolute temperature, and J_0 is the minimum value of ideal reverse saturation current density of the semiconductor energy converter, which is confirmed as $J_0 = 1.5 \times 10^5 \exp(-E_{\rm g}/k_{\rm B}T)$ in units of A/cm^2.[16] Next, the net current density (J) of the battery in the reverse-biased direction is given by

$$J = J_{\rm sc} - J_0\left[\exp\left(\frac{qV}{k_{\rm B}T}\right) - 1\right], \tag{3}$$

where V is the voltage across the resistive load. Based on Eq. (3), the maximum output power density ($P_{\rm max}$) can be induced by

$$\left(1 + \frac{qV_{\rm m}}{k_{\rm B}T}\right)\exp\left(\frac{qV_{\rm m}}{k_{\rm B}T}\right) = 1 + \frac{J_{\rm sc}}{J_0}, \tag{4}$$

where $V_{\rm m}$ is the voltage across the resistive load when $P = P_{\rm max}$ and then the value of $P_{\rm max}$ can be calculated. The fill factor (FF) is given by

$$\text{FF} = \frac{P_{\rm max}}{J_{\rm sc} \cdot V_{\rm oc}}. \tag{5}$$

Finally, there are usually two definitions of energy conversion efficiency in the betavoltaic batteries. One is the device conversion efficiency ($\eta_{\rm dev}$), which is given by

$$\eta_{\rm dev} = \frac{P_{\rm max}}{P_{\rm sur}}, \tag{6}$$

where $P_{\rm sur}$ is the apparent power density entering towards the energy converter. The other is the total conversion efficiency ($\eta_{\rm total}$), which can be separated into the utilization efficiency of the source and the device conversion efficiency of the battery, and is given by

$$\eta_{\rm total} = \frac{P_{\rm max}}{P_{\rm total}} = (1 - \eta_{\rm sel}) \cdot \eta_{\rm dev}, \qquad (7)$$

where $P_{\rm total}$ is the total power density produced in the source, and $\eta_{\rm sel}$ is the self-absorption loss of source. In this study, the total conversion efficiency is calculated by the maximum output power density of one energy converter divided by half the total power density produced in the source. The main reason is that the same energy converters are always settled on each side of the source in a practically fabricated battery.

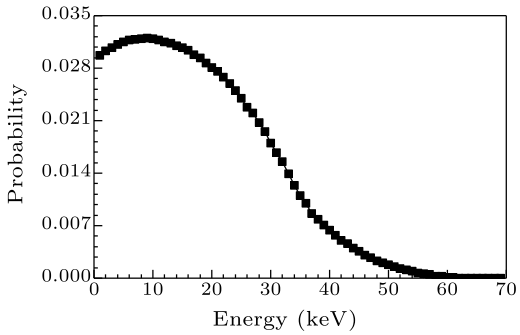

Fig. 3. The energy spectrum of the ^{63}Ni source.

Firstly, the self-absorption effect of the source is researched. The energy spectrum of the ^{63}Ni source is shown in Fig. 3. Based on the simulations, the results in Fig. 4 show that when the thickness of the ^{63}Ni layer increases from 2×10^{-3} μm to 10 μm, the apparent power density increases and nearly reaches the saturation value of 3.24 μW/cm^2 at 2 μm. Then the self-absorption loss ($\eta_{\rm sel}$), which is defined as the ratio of the energy deposited in the source to the total energy produced in the source, increases from 0.036% to 93.7%, and is about 70% when the source thickness is 2 μm. Further calculations show that when the thickness of the ^{63}Ni layer increases from 2×10^{-3} μm to 10 μm, the average energy of the emitted energy spectrum increases from 17.5 keV to 21.24 keV before it reaches the saturation value at about 2 μm. These results can be explained such that when the source is thin, the low-energy beta particles are easy to be absorbed and the high-energy beta particles can emit from the source. However, when the source is thick enough, even high-energy beta particles in deep position can barely emit, both the apparent power density and the emitted energy spectrum remain almost unchanged.

In general, the energy deposited in the air gap and the electrode layer, which exists between the beta source and the energy converter in a betavoltaic battery, is very low.[2] However, the energy loss due to the backscatter electrons on the surface of the battery is significant.[10] Theoretical analysis has shown that the lower the atomic number of the target material is and the smaller the thickness of the sample is, the higher the energy of incident particles contributes to the lower energy backscatter loss. In this study, the energy converter only consists of the diamond material, its geometry structure is cuboid, the source is close to its surface, and the whole device is set in a vacuum. Then as shown in Fig. 5, when the thickness of the ^{63}Ni layer increases from 2×10^{-3} μm to 10 μm, the energy backscatter coefficient ($\eta_{\rm sca}$) on the surface of the diamond material, which is the energy of backscatter electrons divided by the energy entering into the energy converter, decreases from 20% to the minimum value of 12% at about 2 μm.

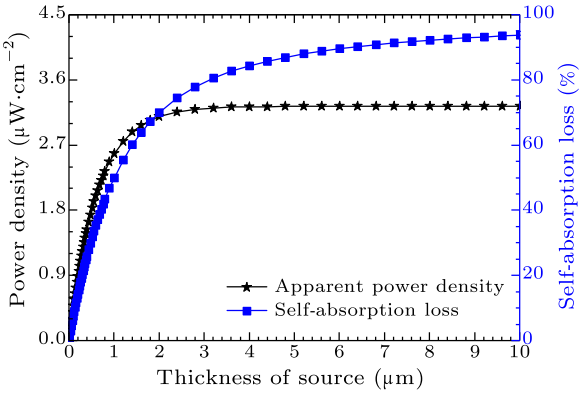

Fig. 4. The apparent power density and the self-absorption loss versus the thickness of the ^{63}Ni source.

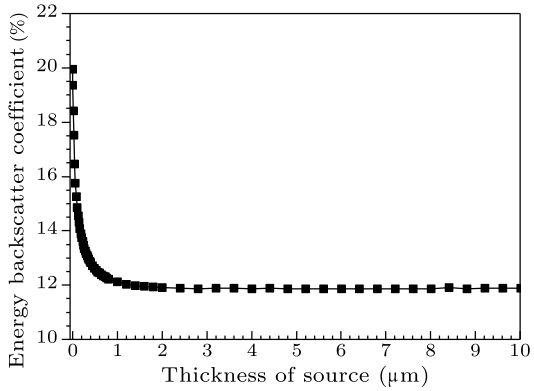

Fig. 5. The energy backscatter coefficient on the surface of the diamond material versus the thickness of the ^{63}Ni source.

In the case of radiation interactions with the solid material, the higher electron density of diamond material contributes to the larger stopping power. Thus a thin diamond absorbed membrane is needed for the energy of the ^{63}Ni source. Firstly, it is obtained that when the thickness of the ^{63}Ni layer increases from 2×10^{-3} μm to 10 μm, the total energy deposited in the diamond energy converter, which represents the maximum available energy for the electron-hole pair generation in the diamond-^{63}Ni battery, increases from 4.2×10^{-3} μW/cm^2 to 1.5 μW/cm^2 before it reaches the saturation value at about 2 μm. Then to achieve the electron-hole pair generation distribution in the energy converter, the energy deposition distribution of the ^{63}Ni source in the diamond material is analyzed. Here for the 0.1-, 0.3-, 0.6-, 1-, 1.6-, 2-, 4-, 6-, and 10-μm-thick sources, the fitting curves in Fig. 6 show that the deposited power density per unit length

(dE/dX) nearly exponentially decreases with the increasing penetration depth (X) in the material. These results mean that the decay energy of the ^{63}Ni source is absorbed quickly in the region, which is close to the surface of the energy converter. Next, as described in Fig. 7, the energy deposition percentage, which is the energy deposited in the region from the surface to a specific depth divided by the total energy deposited in the energy converter, increases and then reaches the maximum value with the increasing penetration depth in the material.

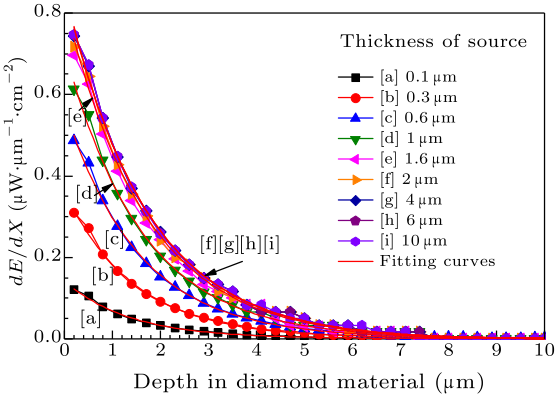

Fig. 6. The deposited power density per unit length versus the depth in the diamond material.

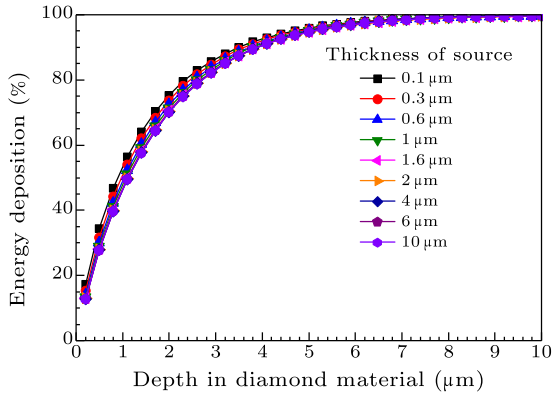

Fig. 7. The energy deposition percentage versus the depth in the diamond material.

Then it is shown that the energy deposition percentage is insensitive to the thickness of the source layer due to the similar emitted energy spectra of sources with various thicknesses. That is to say, the energy deposition distribution is insensitive to the thickness of the source layer. Next, it is achieved that the main energy deposition region, which absorbs above 99% of the total energy deposited in the energy converter, is about 7.7 μm in the diamond-^{63}Ni batteries. Finally, the further calculations show that the maximum penetration depth of the ^{63}Ni source in the diamond material, which is mainly determined by the maximum energy of beta particles, is nearly 22 μm. These results are important for the optimal design of energy converters in the betavoltaic batteries.

Based on the results stated above, the theoretical maxima of electrical properties of the diamond-^{63}Ni batteries are calculated. In the calculations, we assume that the total deposited energy is in the active region of the energy converter and the charge collection efficiency is 100%. As shown in Fig. 8, when the thickness of ^{63}Ni layer increases from 2×10^{-3} μm to 10 μm, the short-circuit current density increases from 2.62×10^{-4} μA/cm^2 to 9.42×10^{-2} μA/cm^2 and the open-circuit voltage increases from 4.6 V to 4.8 V before saturating at about 2 μm.

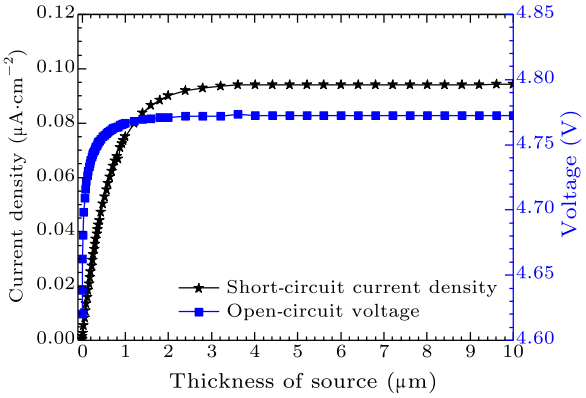

Fig. 8. The short-circuit current density and the open-circuit voltage versus the thickness of the ^{63}Ni source.

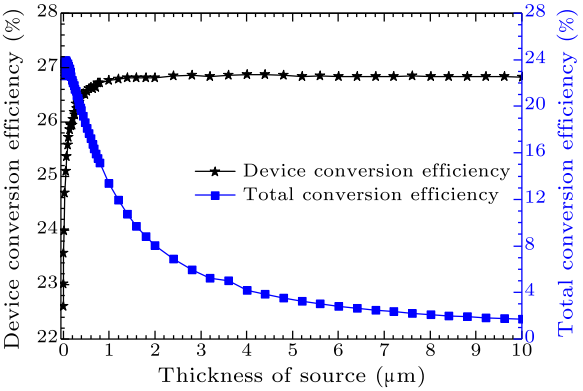

Fig. 9. The energy conversion efficiencies versus the thickness of the ^{63}Ni source.

Compared with the short-circuit current density, the open-circuit voltage is insensitive to the thickness of the ^{63}Ni layer. The main reason is that the reverse saturation current, which is usually much smaller than the short-circuit current, mainly determines the open-circuit voltage and has been reported in the precious experimental tests.[13–15] Then according to Eqs. (3) and (4), it is calculated that when the thickness of the ^{63}Ni layer increases from 2×10^{-3} μm to 10 μm, the theoretical upper limit of the maximum output power density increases from 1.2×10^{-3} μW/cm^2 to the saturation value of 0.42 μW/cm^2 at about 2 μm, and the fill factor increases from 96.4% to the maximum value of 96.7% at about 1 μm.

Finally, the results in Fig. 9 show that when the thickness of the ^{63}Ni layer increases from 2×10^{-3} μm to 10 μm, the theoretical maximum of device conversion efficiency increases from 22.6% to the maximum value of 26.8% at about 2 μm and the total conversion efficiency decreases from 22.6% to 1.7%. Thus the device conversion efficiency of 26.8% is obtained when the thickness of ^{63}Ni source is 6 μm, which is nearly consistent with the value of 29%.[16]

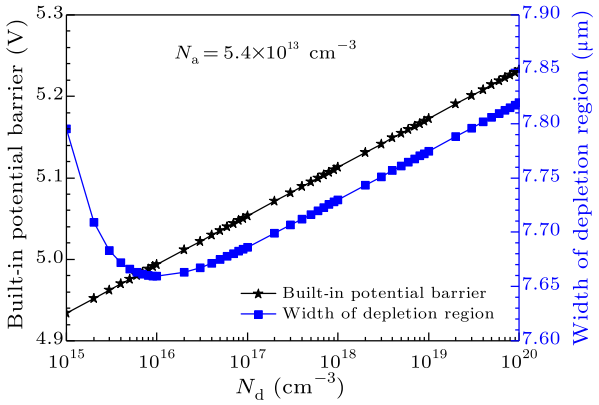

Fig. 10. The width of depletion region and the built-in potential barrier versus the donor doping concentration N_d based on the acceptor doping concentration $N_a = 5.4\times10^{13}/\text{cm}^3$.

For the optimal design of a p–n junction battery, it is most important that the depletion region matches the main ionizing radiation region well. In an ideal p–n homojunction, the width of depletion region (W) at zero bias voltage is given by

$$W = \left\{\frac{2\varepsilon_0\varepsilon_s V_{bi}}{q}\left(\frac{N_a + N_d}{N_a \cdot N_d}\right)\right\}^{1/2}, \tag{8}$$

where ε_0 is the vacuum dielectric constant, ε_s is the relative dielectric constant (5.7 for the diamond material),[2] N_a is the acceptor doping concentration in the p-type doped region, N_d is the donor doping concentration in the n-type doped region, and V_{bi} is the built-in potential barrier, which is given by

$$V_{bi} = \frac{k_B \cdot T}{q} \ln \frac{N_a \cdot N_d}{n_i^2}, \tag{9}$$

with n_i being the intrinsic carrier concentration of the semiconductor material. Then the relationship, which is the width of depletion region extending into the p-type doped region (W_p) and the n-type doped region (W_n) from the metallurgical junction, is expressed as

$$\frac{W_p}{W_n} = \frac{N_d}{N_a}. \tag{10}$$

It is shown that the lower doping concentration results in the larger extending width of the depletion region in the corresponding doped region. Now, for the diamond-^{63}Ni batteries in this study, the depletion region should be equal to or larger than 7.7 μm and it is better to extend into the p-type doped region. Based on Eqs. (8)–(10), it is obtained that when the light acceptor doping concentration in the p-type doped region is $5.4\times10^{13}/\text{cm}^3$, the donor doping concentration in the n-type doped region varies between $2\times10^{15}/\text{cm}^3$ and $5\times10^{18}/\text{cm}^3$, the depletion region is about 7.7 μm and nearly extends into the p-type doped region. Then the built-in potential barrier, which is regarded as the upper limit of open-circuit voltage in a p–n junction battery, increases from 4.95 V to 5.23 V and these values are larger than the theoretical maxima of open-circuit voltage of 4.8 V in the diamond-^{63}Ni batteries. Thus the design of doping concentrations about the diamond-based energy converter is reasonable. These results are plotted in Fig. 10. Next, when the thickness of the source is about 2 μm, the p-type doped region is nearly 7.7 μm and the p^+ layer as the upper electrode layer with the high level doping concentration of $1\times10^{20}/\text{cm}^3$,[13–15] the performance of diamond-^{63}Ni battery based on the $p^+p^-n^+$ junction designed above nearly reaches the theoretical maximum and the results are listed in Table 2. Moreover, the whole thickness of energy converter should be larger than 22 μm to prevent beta particles to escape from the device for ^{63}Ni layers with different thicknesses, and the base metal electrode layer such as Al, Ti, Pt, Au and Ni can be fabricated in a practical battery.

Table 2. The theoretical performance of the cell.

J_{sc}	V_{oc}	P_{max}	FF	η_{dev}	η_{total}
0.09 μA/cm^2	4.8 V	0.42 μW/cm^2	96.7%	26.8%	8%

In summary, the diamond-^{63}Ni p–n junction batteries have been investigated. Firstly, the main factors, which affect the energy conversion efficiencies, are analyzed. Next, the theoretical maxima of electrical properties and the energy conversion efficiencies of the batteries are calculated. Furthermore, a feasible design of the diamond-^{63}Ni battery based on the $p^+p^-n^+$ junction energy converter is presented. These results are helpful for practically fabricated batteries. Finally, although a diamond material and a ^{63}Ni source are used in this study, the calculated model can be used in other semiconductor materials and beta sources in betavoltaic batteries.

References

[1] Oh K et al 2012 *Nucl. Technol.* **179** 234
[2] Prelas M A et al 2014 *Proc. Nucl. Energ.* **75** 117
[3] Sadeghi H et al 2016 *J. Comput. Electron.* **15** 1577
[4] Rahmani F and Khosravinia H 2016 *Radiat. Phys. Chem.* **125** 205
[5] Wang H et al 2015 *Nucl. Instrum. Methods Phys. Res. Sect. B* **359** 36
[6] Chen H Y et al 2011 *J. Phys.* D **44** 215303
[7] Qiao D Y et al 2011 *J. Microelectromech. Syst.* **20** 685
[8] Gui G et al 2016 *Appl. Radiat. Isot.* **107** 272
[9] Thomas C et al 2016 *Appl. Phys. Lett.* **108** 013505
[10] Li F H et al 2014 *Sci. Chin. Technol. Sci.* **57** 25
[11] San H S et al 2013 *Appl. Radiat. Isot.* **80** 17
[12] Lu M et al 2011 *Energy Convers. Manage.* **52** 1955
[13] Bormashov V et al 2015 *Phys. Status Solidi* A **212** 2539
[14] Delfaure C et al 2016 *Appl. Phys. Lett.* **108** 252105
[15] Tarelkin S et al 2016 *Phys. Status Solidi* A **213** 2492
[16] Liu Y P et al 2015 *J. Radioanal. Nucl. Chem.* **304** 517